Egypt. J. Chem. **Vol. 65,** No. SI13B pp. 1553 - 1560 (2022)

Egyptian Journal of Chemistry

http://ejchem.journals.ekb.eg/

Synthesis and *In silico* Docking Study of Some New Quinazolin-2,4-diones Targeting COVID-19 (SARS-Cov-2) Main Protease: A Search for Anti-Covid19 Drug Candidates

Amal O. A. Ibrahim[a], Ahmed M. Mosallam[a], Mohamed M. Taha[a], Hussain Temairk[a], Aboubakr H. Abdelmonsef[a,*]

[a] *Chemistry Department, Faculty of Science, South Valley University, 83523 Qena, Egypt*

Abstract

In the present study, a new series of quinazolin-2,4-dione analogues was synthesized by reaction of 4-(2,4-dioxo-1,4-dihydro-2H-quinazolin-3-yl)-benzoyl chloride **1** with several diamines in presence of triethyl amine (TEA) and dioxane. The newly compounds **2-6** were structurally confirmed by means of spectral techniques such as IR, ^{1}H-NMR, ^{13}C-NMR, MS and elemental analysis. Moreover, an *in silico* molecular docking analysis of the newly compounds was performed to identify new potential therapeutic agents against Covid-19, targeting main protease (Mpro) enzyme. Compound **4** exhibited the highest binding affinity against the selected target. In addition, *in silico* drug-likeness and ADMET (absorption, distribution, metabolism, excretion, and toxicity) findings exhibited that compound **4** obeyed Lipinski's rule of five (Ro5) and could be used as drug candidate to combat Covid-19 disease.

Keywords: quinazolin-2,4-dione; molecular docking; covid-19; binding affinity.

1. Introduction

Coronavirus disease-2019 (COVID-19), a viral disease caused by severe acute respiratory syndrome coronavirus-2 (SARS-CoV2) was showed a global pandemic by WHO in 2020 [1]. Novel coronavirus SARS-CoV2 causes COVID-19, an epidemic threatening millions of peoples [2], [3]. As protective immunity does not present in humans, the virus is able to escape innate immune responses, it can mushroom, unhindered, in initially infected tissues [4]. Consecutive cell death leads to the release of virus particles and intracellular components to the extracellular area, which leads to immune cell mobilization, the generation of immune complexes and related damage [5].

Quinazolin-2,4-diones [6]–[9] are a class of fused heterocyclic compounds which have considerable interest because of the wide range of their applications in medicinal and pharmaceutical applications [10], [11] as antiviral [12], anti-cancer [13], anti-malarial [14], anti-inflammatory [15], anti-cholera agents [16].

In continuation with our work in the design and synthesis of new series of quinazolin-2,4-dione analogues, herein, the synthesis of new bioactive compounds containing the quinazolin-2,4-dione skeleton **2-6** was performed by reaction of 4-(2,4-dioxo-1,4-dihydro-2H-quinazolin-3-yl)-benzoyl chloride **1** with diamines namely, *o*-phenylene diamine, *p*-phenylene diamine, and/or benzidine in presence of TEA and dioxane. Moreover, *in silico* molecular docking approach of the compounds [17]–[24] was carried out to predict their binding affinities and mode of actions against COVID-19 Mpro. Finally, ADMET profile and physiochemical properties of the ligand molecules were calculated using different tools such as SwissADME, AdmetSAR, and Mol inspiration.

2. Experimental

2.1. Chemistry

2.1.1 Instruments

The melting points of the afforded compounds were determined using Griffin apparatus and are uncorrected. The purity of the newly prepared derivatives **2-6** is monitored by Thin Layer Chromatography TLC technique. IR spectrum was recorded on Shimadzu 408 and Bruker Vect. 22. ^{1}H-NMR and ^{13}C-NMR spectra were recorded in DMSO-d_6 solutions on BRUKER 400 FT-NMR spectrometer, and chemical shifts are expressed in ppm units using TMS as an internal reference. The

*Corresponding author e-mail: aboubakr.ahmed@sci.svu.edu.eg.; (Aboubakr Ahmed).
Receive Date: 20 January 2022, Revise Date: 21 February 2022, Accept Date: 08 March 2022
DOI: 10.21608/EJCHEM.2022.117407.5296

chemical shifts were measured in ppm (δ) related to TMS (0.00 ppm). Finally, mass spectrum was recorded on a HP model, Mass 5988 Mass spectrometer at 70 eV. All the synthesized compounds were analyzed for C, H, and N at Cairo University, Egypt.

2.1.2 Synthesis of quinzolin-2,4-dione derivatives

2.1.2.1 4-(2,4-dioxo-1,4-dihydro-2H-quinazolin-3-yl)-benzoyl chloride 1

4-(2,4-dioxo-1,4-dihydro-2H-quinazolin-3-yl)-benzoic acid (0.013 mol, 1 gm) was dissolved in thionyl chloride, then the reaction mixture was refluxed for 5 hrs. After completion of the reaction, the excess of thionyl chloride was evaporated (b.p. 74.6 °C) by concentration the reaction mixture, then the residue was allowed to stand at room temperature, then recrystallized from benzene/ethanol to yield the product 4-(2,4-dioxo-1,4-dihydro-2H-quinazolin-3-yl)-benzoyl chloride **1** as yellow crystal. Yield: 85 %. M.P: 270 ºC. FT-IR (KBr, υ, cm^{-1}) = 3195 (NH), 1763, 1725 (C=O's), 1630 (C=C), 751 (C-Cl). ^{1}H-NMR (DMSO-d_6, 400 MHz): δ (ppm) =11.65 (s, 1H, NH), 7.22-8.07 (m, 8H, Ar-H). ^{13}C-NMR (DMSO-d_6, 100 MHz): δ 114.74, 115.77, 123.09, 127.52, 128.04, 129.99, 130.30, 131.95, 135.81, 140.30, 150.43, 162.57, 167.35. MS (EI): *m/z* (%) =300 $[M]^+$, 302 $[M]^+$+2. Anal. Calcd for $C_{15}H_9ClN_2O_3$: C, 59.91; H, 3.02; Cl, 11.79; N, 9.32%. Found C, 60.16; H, 3.26; Cl, 11.84; N, 9.18%.

2.1.2.2 3-[4-(1H-benzo-imidazol-2-yl)-phenyl]-1H-quinazolin-2,4-dione 2

To *o*-phenylenediamine (0.003 mol, 0.36 gm) in acetone (10 ml), 4-(2,4-dioxo-1,4-dihydro-2H-quinazolin-3-yl)-benzoyl chloride **1** (0.003 mol, 1 gm) was added. Then the reaction mixture was stirred at room temperature for 2 hrs until completion of the reaction, which was indicated by TLC. The resulting solid was filtered off then recrystallized from methanol to afford compound **2**, as pale brown crystals. Yield: 75%. M.P: > 300 ºC. FT-IR (KBr, υ, cm^{-1}): 3427, 3244 (NH's), 1724, 1668 (C=O's), 1615 (C=C), 1605 (C=N). ^{1}H-NMR (DMSO–d_6, 400 MHz): δ (ppm)= 11.63 (s, 1H, NH), 10.19 (s, 1H, NH), 7.23-8.09 (m, 12H, Ar-H). MS (El): *m/z* (%)= 353.9 $[M]^+$. Anal. Calcd for $C_{21}H_{14}N_4O_2$ (Mol. Wt.: 354): C, 71.18; H, 3.98; N, 15.81%, found: C, 71.37; H, 4.09; N, 15.90%.

2.1.2.3 General procedures for the synthesis of arylquinazolin-2,4-diones 3-6

Reaction of 4-(2,4-dioxo-1,4-dihydro-2H-quinazolin-3-yl)-benzoyl chloride **1** with *p*-phenylenediamine (1:1 and/or 1:2 molar ratio) in dioxane (20 ml) and few drops of TEA afforded compounds **3** and/or **4**, respectively.

N-(4-amino-phenyl)-4-(2,4-dioxo-1,4-dihydro-2H-quinazolin-3-yl)-benzamide 3: brown crystals. Yield: 70%. M.P: > 300 ºC. FT-IR (KBr, υ, cm^{-1}): 3313, 3300 (NH_2), 3062 (NH), 1723, 1662 (C=O's), 1590 (C=C). ^{1}H-NMR (DMSO–d_6, 400 MHz): δ (ppm)= 11.68 (s, 1H, NH), 10.44 (s, 1H, NH), 7.02-8.08 (m, 12H, Ar-H), 3.59 (s, 2H, NH2). ^{13}C-NMR (DMSO–d_6, 100 MHz): δ 112.0, 114.1, 114.9, 116.6, 117.3, 127.9, 128.2, 128.4, 129.1, 133.5, 135.4, 137.4, 139.7, 148.4, 150.0, 161.2, 164.7. MS (El): *m/z* (%)= 372 $[M]^+$. Anal. Calcd for $C_{21}H_{16}N_4O_3$ (Mol. Wt.: 372): C, 67.73; H, 4.33; N, 15.05%, found: C, 67.86; H, 4.54; N, 15.13%.

N,N'-(1,4-phenylene)bis(4-(2,4-dioxo-1,4-dihydroquinazolin-3(2H)-yl)benzamide) 4: grey crystals. Yield: 80 %. M.P: >300 ºC. FT-IR (KBr, υ, cm^{-1}): 3357 (NH), 1725, 1658 (C=O's), 1617 (C=C). ^{1}HNMR (DMSO–d_6, 400MHz): δ (ppm)= 11.64 (s, 2H, 2NH-quinazoline), 10.24 (s, 2H, 2NH), 6.90-8.04 (m, 10H, Ar-H). ^{13}C-NMR (DMSO–d_6, 100 MHz): δ 114.76, 115.78, 117.57, 122.36, 123.03, 128.06, 128.57, 129.65, 135.44, 135.81, 138.85, 140.32, 150.51, 162.64, 165.15. MS (El): *m/z* (%)= 637 $[M]^+$+1. Anal. Calcd for $C_{36}H_{24}N_6O_6$ (Mol. Wt.: 636): C, 67.92; H, 3.80; N, 13.20%, found: C, 67.66; H, 3.68; N, 13.08%.

Reaction of **1** with benzidine (1:1 and/or 1:2 molar ratio) in dioxane (20 ml) and few drops of TEA afforded compounds **5** and/or **6**, respectively.

N-(4'-amino-biphenyl-4-yl)-4-(2,4-dioxo-1,4 dihydro-2H-quinazolin-3-yl)-benzamide 5: pale yellow crystals. Yield: 75 %. M.P: 290 ºC. FT-IR (KBr, υ, cm^{-1}): 3342, 3360 (NH_2), 3063 (NH), 1724, 1656 (C=O's), 1580 (C=C). ^{1}H-NMR (DMSO–d_6, 400 MHz): δ (ppm)= 11.64 (s, 1H, NH), 10.46 (s, 1H, NH), 7.09-8.07 (m, 16H, Ar-H and NH_2). ^{13}C-NMR (DMSO–d_6, 100 MHz): δ 112.0, 114.3, 114.9, 117.3, 127.1, 127.9, 128.2, 128.4, 129.1, 133.5, 135.4, 137.4, 138.9, 139.7, 148.4, 150.0, 161.2, 164.7. MS (El): *m/z* (%)= 448 $[M]^+$. Anal. Calcd for $C_{27}H_{20}N_4O_3$ (Mol. Wt.: 448): C, 72.31; H, 4.49; N, 12.49%, found: C, 72.40; H, 4.35; N, 12.38%.

N,N'-([1,1'-biphenyl]-4,4'-diyl)bis(4-(2,4-dioxo-1,4-dihydroquinazolin-3(2H)-yl)benzamide) 6: brown crystals. Yield: 70 %. M.P: >300 ºC. FT-IR (KBr, υ, cm^{-1}): 3287 (NH), 1731, 1652 (C=O's), 1600 (C=C). ^{1}HNMR (DMSO–d_6, 400 MHz): δ (ppm)= 11.64 (s, 2H, 2NH-quinazoline), 10.48 (s, 2H, 2NH), 7.27-8.06 (m, 24H, Ar-H). ^{13}C-NMR (DMSO–d_6, 100 MHz): δ 112.0, 114.9, 117.3, 117.9, 127.1, 127.9, 128.2, 128.4, 129.1, 133.5, 135.4, 137.4, 138.9, 139.7, 148.4, 150.0, 161.2, 164.7. MS (El): *m/z* (%)= 712 $[M]^+$. Anal. Calcd for $C_{42}H_{28}N_6O_6$ (Mol. Wt.: 712): C, 70.78; H, 3.96; N, 11.79%, found: C, 70.82; H, 4.06; N, 11.68%.

2.2 Molecular docking and ADMET analysis

The crystal structure of the target Mpro was selected from RSCB protein data bank. The pdb file

was then prepared and energy minimized using CHARMM Force Field [30]. The pdbqt file for Mpro target was prepared according to PyRx protocol. The docking grid was set to 25 Å × 25 Å × 25 Å. The grid center was positioned at the center of the active site of Mpro. The chemical structures of the synthesized compounds were generated using ChemDraw 8.0, and their 3D structures were generated using Open Babel 2.4.1 tool [31]. All compounds were then energetically minimized using UFF Force Field [32]. Molecular docking calculations [33]–[35] were carried out using PyRx–virtual screening software. As well, the lowest energy conformation from the largest cluster was picked out as a representative binding pose [3]. Moreover, ADMET profile and physiochemical properties of the ligand molecules were calculated using free access tools namely, SwissADME, AdmetSAR, and Mol inspiration.

2. Results and discussion

3.1. Chemistry

The synthetic protocol adopted in this study is illustrated in **Scheme 1**. Compound **1** was obtained by reaction of 4-(2,4-dioxo-1,4-dihydro-2H-quinazolin-3-yl)-benzoic acid with thionyl chloride under solvent-free conditions. The chemical structure of compounds **1** was confirmed by spectral analysis. Nuclear magnetic resonance (^{1}H-NMR) showed singlet signal for NH proton at δ 11.65 ppm, in addition to multiplet signals which related to aromatic protons at δ 7.22-8.07 ppm. The mass spectrum of compound **1** is shown in **Figure 1**. In addition, compound **2** was prepared by stirring of compound **1** with *o*-phenylenediamine at room temperature in acetone for 2 hrs. Moreover, compounds **3-6** were synthesized by the nucleophilic reaction of compound **1** with *p*-phenylenediamine and/or benzidine in different molar ratios (1:1, and/or 1:2), in dioxane with few drops of TEA for 3-6 hrs. The chemical structures of the newly compounds **2-6** were approved by their spectral and elemental analyses. IR spectra of derivatives **2**, **4**, and **6** approved by valuable information about nature of functional group present in these derivatives. The absorption bands at 3437, and 3296 cm^{-1} suggested the presence of NH's, while 1726, and 1659 cm^{-1} attributed to presence of C=O's. On the other hand, the band at 1605 cm^{-1} suggested the presence of C=N groups in compound **2**. Also, ^{1}H-NMR confirmed the structures, by appearance of singlet peak at δ 11.63, 10.30 ppm corresponding to two NH groups of quinazoline moiety and NH amidic, respectively. In addition, the aromatic protons (Ar-H) appeared at the region of δ 6.90-8.06 ppm.

On the other hand, IR spectra for compounds **3**, and **5** exhibited the characteristic bands at 3333 cm^{-1} for NH_2, at 3063, 2958 cm^{-1} for NH's, and at 1723, 1659 cm^{-1} for C=O's groups. Additionally, ^{1}H-NMR spectrum showed characteristic peaks as singlet at δ 11.66 and 10.45 ppm attributed to protons of NH's groups, in addition a multiplet signals at δ 7.05-8.07 ppm for aromatic protons, also appearance of singlet signal at δ 3.59 ppm for (NH_2) protons.

3.2. Computational study

In the present study, Covid-19 Mpro was selected as therapeutic target for identification of potential drug candidates for coronavirus treatment. The crystallographic structure of the target protein was retrieved from the RCSB Protein Data Bank web server (PDB ID: 7bqy) [25], with resolution of 1.7 Å. All the prepared compounds 2-6 were docked into the active site of the target by using PyRx-virtual screening tool [26]. The binding affinities of the docked molecules to the target protein are represented in **Table 1**. The molecular docking analysis exhibited that the amide fragment and quinazoline moiety can act as hydrogen bond donors/acceptors to generate hydrogen bond interactions as represented below. **Figure 2** showed the 2D and 3D representations of all docked compounds with the target Mpro. Compounds docked to the target enzyme and exhibited binding energies in the range of -7.9 to -9.6 kcal/mol. As represented in **Table 1**, compound **4** exhibited the best binding energy (-9.6 kcal/mol) against Mpro and showed one H-bond and two arene-cation interactions with the residues GLN127, LYS5, and LYS137 at distances of 2.99, 3.77, and 5.78 Å, respectively. The other compounds also docked with the target enzyme through various types of interactions such as H-bonds and arene-stacking.

On the other hand, ADMET profile of the newly prepared compounds was predicted as presented in **Table 2**. The findings clearly showed that they can be absorbed by the intestine, as their molecular weights were in the acceptable range (≤725 g/mol). *In silico* absorption percentage calculations showed high absorption percentage values (98–100%). Hence, we can conclude that compounds possess good absorption and distribution properties [27], [28]. Additionally, their TPSA values were in the acceptable range (below 140 A^2), indicating that the compounds had considerable permeability into the plasma membrane [29]. Moreover, number of violations of Lipinski's rule of five is zero, indicating drug-likeness properties.

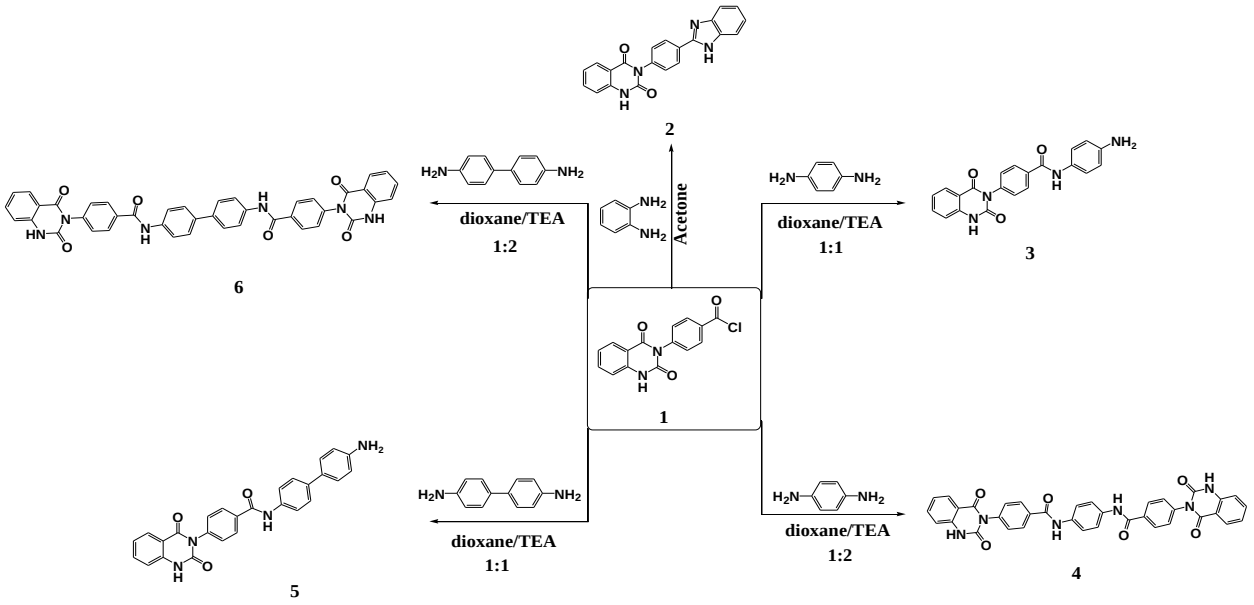

Scheme 1. Synthetic routes of quinazolin-2,4-dione skeletons 2-6

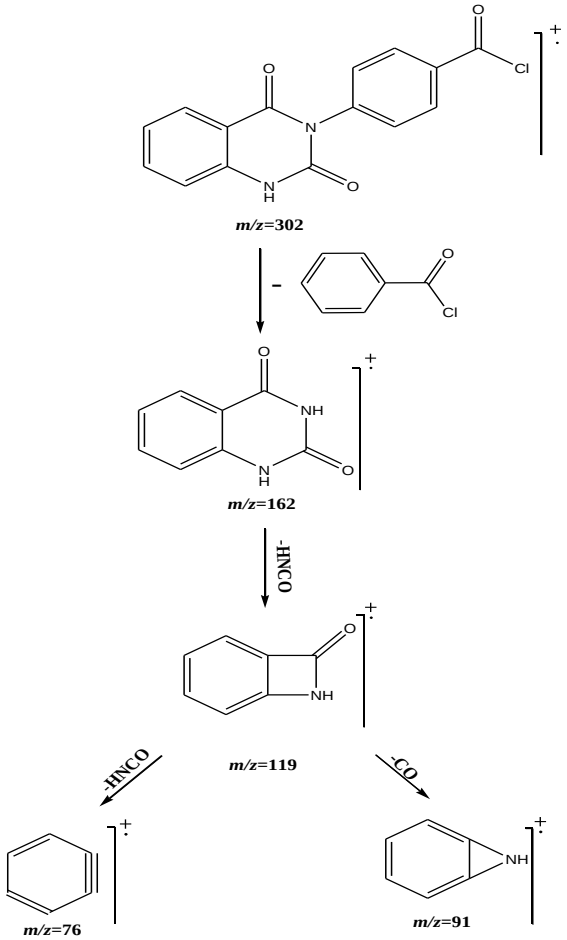

Figure 1. Mass fragmentation of compound 1

Table 1.

Binding energies and molecular interactions between the docked compounds **2-6** and the target Mpro

	Binding Energy kcal/ mol	Docked complex (amino acid–ligand) interactions	Distance (Å)
2	-8.2	**H-bonds**	
		LYS137:NZ—compound 2	1.86
		THR199:OG1—compound 2	2.95
		ASP289:N—compound 2	3.00
		arene-cation	
		ARG131:NH1—compound 2	5.00
		ARG131:NH2—compound 2	5.24
3	-7.9	**H-bonds**	
		LYS137:NZ —compound 3	3.10
		THR199:OG1 —compound 3	2.39
		LEU287:N—compound 3	2.14
		arene-cation	
		ARG131:NH1—compound 3	5.17
		LYS137:NZ—compound 3	3.90
4	-9.6	**H-bonds**	
		GLN127:N —compound 4	2.99
		arene-cation	
		LYS5:NZ—compound 4	3.77
		LYS137:NZ—compound 4	5.78
5	-8.6	**H-bonds**	
		LYS137:NZ —compound 5	2.88
		THR199:OG1 —compound 5	2.81
		LEU271:N—compound 5	2.99
		arene-cation	
		LYS137:NZ—compound 5	4.17
6	-9.2	**arene-cation**	
		ARG40:NH1—compound 6	4.76
		arene-sigma	
		ASN84:CA—compound 6	3.53

Table 2.

ADMET profile and drug-likeness properties of the docked molecules **2-6**

	Molecular Weight (g/mol)	Blood-Brain Barrier (BBB+)	Caco-2 Permeability (Caco2+)	%Human Intestinal Absorption (HIA+)	logp	TPSA A^2	HBA	HBD	N rotatable	N violations	AMES toxicity	Carcinogenicity
acceptable ranges	**130–725**	**-3 to 1.2**	**<25 poor 500 great**	**>80% high <25% low**	**<5**	**≤140**	**2.0–20.0**	**0.0–6.0**	**≤10**	**≤1**	**Nontoxic**	**Noncarcinogenic**
2	354.36	0.99	54.57	100.00	3.67	83.54	3	2	2	0	Nontoxic	Noncarcinogenic
3	372.38	0.98	52.15	99.49	2.94	109.98	3	3	4	0	Nontoxic	Noncarcinogenic
4	636.61	0.96	52.76	98.02	3.87	97.65	6	4	8	0	Nontoxic	Noncarcinogenic
5	448.47	0.98	52.15	99.49	4.00	109.98	3	3	5	0	Nontoxic	Noncarcinogenic
6	712.71	0.96	52.76	98.02	4.72	97.65	6	4	9	0	Nontoxic	Noncarcinogenic

HBA, number of hydrogen bond acceptors; HBD, number of hydrogen bond donors; logp, logarithm of partition coefficient between n-octanol and water; n rotatable, number of rotatable bonds; TPSA, topological polar surface area.

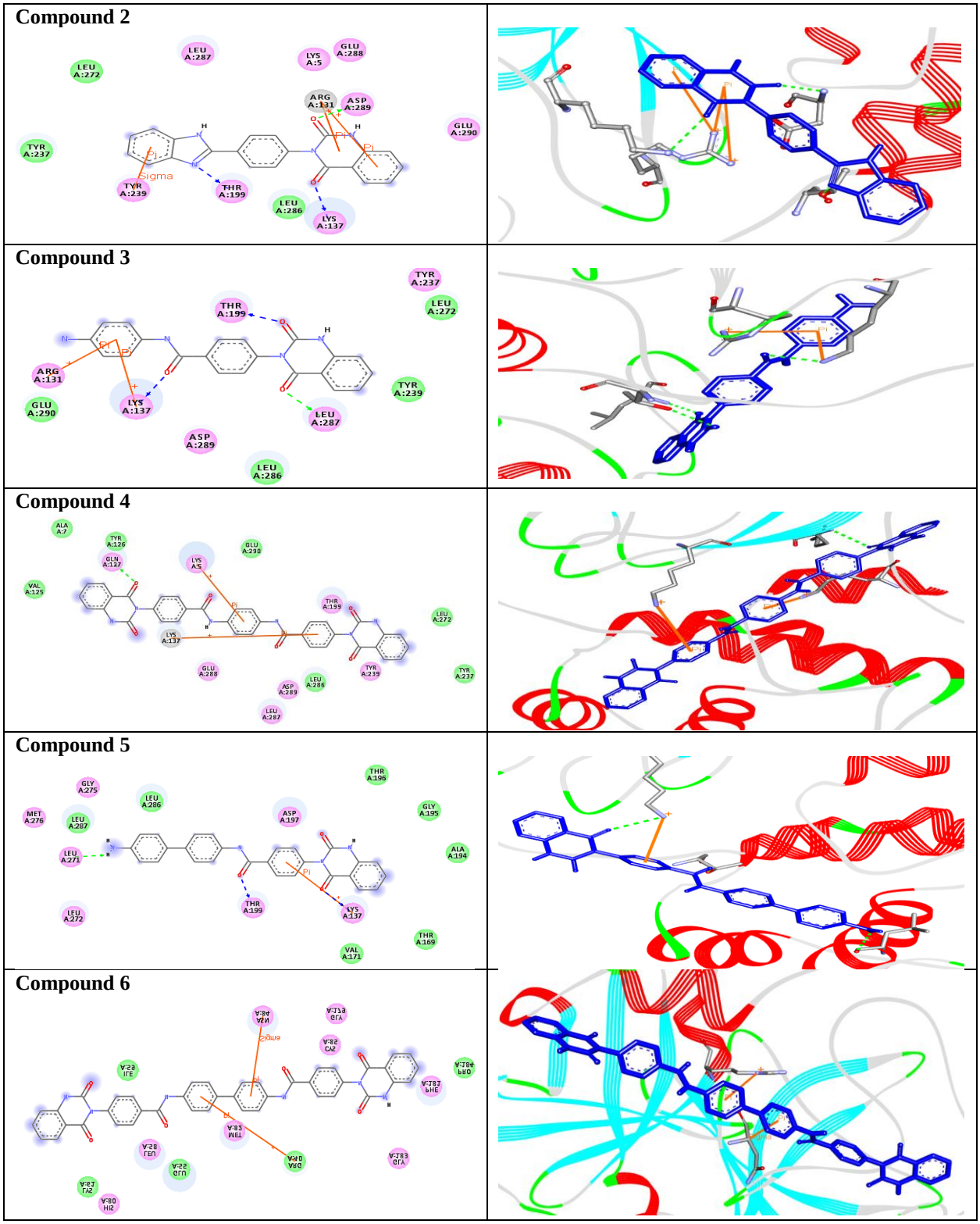

Figure 2. (left side) 2D, and (right side) 3D representations of intermolecular interactions of compounds 2-6 and Mpro

4. Conclusion

In this work, a new series of quinazolin-2,4-dione analogues **2-6** was synthesized starting from 4-(2,4-dioxo-1,4-dihydro-2H-quinazolin-3-yl)-benzoyl chloride **1** with several diamines, namely o- and/or p-phenylenediamine, and benzidine. Their chemical structures were characterized by IR, ^{1}H-, ^{13}C-NMR, MS and elemental analysis. In addition, *in silico* molecular docking technique was performed to identify potential inhibitors against Covid-19, by targeting Mpro enzyme. The study exhibited good binding energies for all compounds against the target enzyme ranging from -7.9 to -9.6 kcal/mol. Compound **4** with the highest binding energy could be considered as promising scaffold for design novel inhibitors for Covid-19 disease.

5. Conflicts of interest

There are no conflicts to declare.

6. References

[1] C. Liu et al., "Research and Development on Therapeutic Agents and Vaccines for COVID-19 and Related Human Coronavirus Diseases," ACS Cent. Sci., 2020, doi: 10.1021/acscentsci.0c00272.

[2] S. Baloch, M. A. Baloch, T. Zheng, and X. Pei, "The coronavirus disease 2019 (COVID-19) pandemic," Tohoku J. Exp. Med., vol. 250, no. 4, pp. 271–278, 2020.

[3] H. R. M. Rashdan, T. A. Yousef, A. H. Abdelmonsef, and M. M. Abou-krisha, "Synthesis and Identification of Novel Potential Thiadiazole Based Molecules Containing 1,2,3-triazole Moiety Against COVID-19 Main Protease Through Structure-Guided Virtual Screening Approach," Biointerface Res. Appl. Chem., vol. 12, no. 6, pp. 8258–8270, Dec. 2021, doi: 10.33263/BRIAC126.82588270.

[4] T. Opriessnig and Y. Huang, "Coronavirus disease 2019 (COVID-19) outbreak: Could pigs be vectors for human infections?," Xenotransplantation, vol. 27, no. 2, 2020.

[5] S. Chauhan, "Comprehensive review of coronavirus disease 2019 (COVID-19)," Biomed. J., vol. 43, no. 4, pp. 334–340, 2020.

[6] M. A. Hassan et al., "NEW QUINAZOLIN-2,4-DIONES FROM (2,4-DIOXO-1,4-DIHYDRO-2H-QUINAZOLIN-3-YLAMINO) ACETIC ACID HYDRAZIDE," 2014.

[7] H. Mohamed Dardeer and A.-B. Haredi Abdel-Monsef, "Novel Routes to Quinazolin-2,4-dione and Benzopyrimidino [4,5-b]naphthalen-2,4-dione Derivatives," J. Pharm. Res., vol. 8, no. 4, pp. 633–637, 2014, [Online]. Available: www.jpronline.info.

[8] M. A. Hassan, A. M. M. Younes, M. M. Taha, S. M. Abboudy, and A. B. H. Abdel-Monsef, "New quinazolin-2,4-diones from (2,4-dioxo-1,4-dihydro-2H- quinazolin -3-ylamino) acetic acid hydrazide," Int. J. Pharm. Pharm. Sci., vol. 6, no. SUPPL. 2, pp. 511–514, 2014.

[9] A. H. Abdelmonsef et al., "A search for antiinflammatory therapies: Synthesis, in silico investigation of the mode of action, and in vitro analyses of new quinazolin-2,4-dione derivatives targeting phosphodiesterase-4 enzyme," J. Heterocycl. Chem., vol. 1, pp. 1–19, Oct. 2021, doi: https://doi.org/10.1002/jhet.4395.

[10] H. S. El-Sheshtawy, A. H. Abdelmonsef, S. M. Abboudy, A. M. M. Younes, M. M. Taha, and M. A. Hassan, "Synthesis, Structural, and Theoretical Studies of Quinazoline-2,4-dione Derivatives," Polycycl. Aromat. Compd., vol. 39, no. 3, pp. 279–286, May 2017, doi: 10.1080/10406638.2017.1325747.

[11] D. Wang and F. Gao, "Quinazoline derivatives: synthesis and bioactivities," Chem. Cent. J., vol. 7, no. 1, p. 95, Dec. 2013, doi: 10.1186/1752-153X-7-95.

[12] V. Alagarsamy, K. Chitra, G. Saravanan, V. R. Solomon, M. T. Sulthana, and B. Narendhar, "An overview of quinazolines: Pharmacological significance and recent developments," Eur. J. Med. Chem., vol. 151, pp. 628–685, May 2018, doi: 10.1016/j.ejmech.2018.03.076.

[13] A. H. Abdelmonsef and A. M. Mosallam, "Synthesis, in vitro biological evaluation and in silico docking studies of new quinazolin-2,4-dione analogues as possible anticarcinoma agents," J. Heterocycl. Chem., pp. 1–18, 2020, doi: 10.1002/jhet.3889.

[14] A. Haredi Abdelmonsef, M. Eldeeb Mohamed, M. El-Naggar, H. Temairk, and A. Mohamed Mosallam, "Novel Quinazolin-2,4-Dione Hybrid Molecules as Possible Inhibitors Against Malaria: Synthesis and in silico Molecular Docking Studies," Front. Mol. Biosci., vol. 7, no. 105, pp. 1–19, Jun. 2020, doi: 10.3389/fmolb.2020.00105.

[15] A. H. Abdelmonsef et al., "A search for antiinflammatory therapies: Synthesis, in silico investigation of the mode of action, and in vitro analyses of new quinazolin-2,4-dione derivatives targeting phosphodiesterase-4 enzyme," J. Heterocycl. Chem., vol. 1, pp. 1–19, Nov. 2021, doi: 10.1002/jhet.4395.

[16] M. El-Naggar, M. E. Mohamed, A. M. Mosallam, W. Salem, H. R. Rashdan, and A. H. Abdelmonsef, "Synthesis, Characterization, Antibacterial Activity, and Computer-Aided Design of Novel Quinazolin-2,4-dione Derivatives as Potential Inhibitors Against Vibrio cholerae," Evol. Bioinforma., vol. 16, pp. 1–13, Jan. 2020, doi: 10.1177/1176934319897596.

[17] E. A. Hassan, I. A. Shehadi, A. M. Elmaghraby, H. M. Mostafa, S. E. Zayed, and A. H. Abdelmonsef, "Synthesis, Molecular Docking Analysis and in Vitro Biological Evaluation of Some New Heterocyclic Scaffolds-Based Indole Moiety as Possible Antimicrobial Agents," Front. Mol. Biosci., vol. 8, pp. 1–17, Jan. 2022, doi: 10.3389/fmolb.2021.775013.

[18] A. Haredi Abdelmonsef, "Computer-aided identification of lung cancer inhibitors through homology modeling and virtual screening," Egypt. J. Med. Hum. Genet., vol. 20, no. 1, Dec. 2019, doi: 10.1186/s43042-019-0008-3.

[19] A. A. Noser, M. El-Naggar, T. Donia, and A. H. Abdelmonsef, "Synthesis, In Silico and In Vitro Assessment of New Quinazolinones as Anticancer Agents via Potential AKT Inhibition," Molecules, vol. 25, no. 20, p. 4780, Oct. 2020, doi: 10.3390/molecules25204780.

[20] H. Rashdan, I. Shehadi, and A. H. Abdelmonsef, "Synthesis, Anticancer Evaluation, Computer-Aided Docking Studies, and ADMET Prediction of 1,2,3-Triazolyl-Pyridine Hybrids as Human Aurora B Kinase Inhibitors," ACS Omega, vol. 6, no. 2, pp. 1445–1455, doi: 10.1021/acsomega.0c05116.

[21] H. R. M. Rashdan, M. El-Naggar, and A. H. Abdelmonsef, "Synthesis, molecular docking studies and in silico admet screening of new heterocycles linked thiazole conjugates as potent anti-hepatic cancer agents," Molecules, vol. 26, no. 6, pp. 1–17, 2021, doi: 10.3390/molecules26061705.

[22] A. M. Abo-Bakr, H. M. Alsoghier, and A. H. Abdelmonsef, "Molecular Docking, Modeling, Semiempirical Calculations Studies and In Vitro Evaluation of New Synthesized Pyrimidin-imide Derivatives," J. Mol. Struct., p. 131548, 2021, doi: https://doi.org/10.1016/j.molstruc.2021.131548.

[23] I. A. Shehadi, H. R. M. Rashdan, and A. H. Abdelmonsef, "Homology modeling and virtual screening studies of antigen MLAA-42Protein: Identification of noveldrugcandidates against leukemia-an in silico approach," Comput. Math. Methods Med., vol. 2020, 2020, doi: 10.1155/2020/8196147.

[24] A. A. Noser, A. H. Abdelmonsef, M. El-naggar, and M. M. Salem, "New Amino Acid Schiff Bases as Anticancer Agents via Potential Mitochondrial Complex I-Associated Hexokinase Inhibition and Targeting AMP-Protein Kinases/mTOR Signaling Pathway," Molecules, vol. 26, no. 5332, pp. 1–27, 2021, doi: https://doi.org/10.3390/molecules26175332.

[25] Z. Jin et al., "Structure of Mpro from SARS-CoV-2 and discovery of its inhibitors," Nature, vol. 582, no. 7811, pp. 289–293, 2020, doi: 10.1038/s41586-020-2223-y.

[26] Dallakyan S and Olson A.J, "Small-Molecule Library Screening by Docking with PyRx," in Chemical Biology, vol. 1263, springer, 2015, pp. 243–250.

[27] Rashdan HRM, Abdelmonsef AH, Shehadi IA, Gomha SM, Soliman AMM, and Mahmoud HK, "Synthesis, Molecular Docking Screening and Anti-Proliferative Potency Evaluation of Some New Imidazo[2,1-b]Thiazole Linked Thiadiazole Conjugates," Molecules, vol. 25, no. 21, p. 4997, 2020, doi: 10.3390/molecules25214997.

[28] Gomha SM et al., "Thiazole-Based Thiosemicarbazones : Synthesis , Cytotoxicity Evaluation and Molecular Docking Study," Drug Des. Devel. Ther., vol. 2021, no. 15, pp. 659–677, 2021, doi: https://doi.org/10.2147/DDDT.S291579.

[29] A. M. El-Maghraby and A. H. Abdelmonsef, "Synthesis, characterization and in silico molecular docking studies of novel chromene derivatives as Rab23 inhibitors," Egypt. J. Chem., vol. 63, no. 4, pp. 1341–1358, 2020, doi: 10.21608/ejchem.2019.15013.1911.

[30] B. R. Brooks et al., "CHARMM: Molecular dynamics simulation package," J. Comput. Chem., vol. 30, no. 10, pp. 1545–1614, 2009, doi: 10.1002/jcc.21287.

[31] N. M. O'Boyle, M. Banck, C. A. James, C. Morley, T. Vandermeersch, and G. R. Hutchison, "Open Babel: An Open chemical toolbox," J. Cheminform., vol. 3, no. 10, p. 33, 2011, doi: 10.1186/1758-2946-3-33.

[32] A. K. Rappé, C. J. Casewit, K. S. Colwell, W. A. Goddard, and W. M. Skiff, "UFF, a Full Periodic Table Force Field for Molecular Mechanics and Molecular Dynamics Simulations," J. Am. Chem. Soc., vol. 114, no. 25, pp. 10024–10035, 1992, doi: 10.1021/ja00051a040.

[33] Abdelmonsef AH, Dulapalli R, Dasari T, Padmarao LS, Mukkera T, and Vuruputuri U, "Identification of Novel Antagonists for Rab38 Protein by Homology Modeling and Virtual Screening," Comb. Chem. High Throughput Screen., vol. 19, no. 10, pp. 1–18, 2016, doi: 10.2174/1386207319666161026153237.

[34] T. Dasari et al., "Design of novel lead molecules against RhoG protein as cancer target – a computational study," J. Biomol. Struct. Dyn., vol. 35, no. 14, pp. 3119–3139, Oct. 2017, doi: 10.1080/07391102.2016.1244492.

[35] Rondla R, PadmaRao LS, Ramatenki V, Haredi-Abdel-Monsef A, Potlapally SR, and Vuruputuri U, "Selective ATP competitive leads of CDK4: Discovery by 3D-QSAR pharmacophore mapping and molecular docking approach," Comput. Biol. Chem., vol. 71, pp. 224–229, Dec. 2017, doi: 10.1016/j.compbiolchem.2017.11.005.